



Alpha Lactose Monohydrate Morphology: Molecular Modelling and Experimental Approach

Zulfahmi Lukman, Nornizar Anuar*, Noor Fitrah Abu Bakar, Norazah Abdul Rahman

Faculty of Chemical Engineering, Universiti Teknologi MARA, 40450 Shah Alam, Selangor, MALAYSIA

*Corresponding author E-mail: nornizar@salam.uitm.edu.my

Abstract

This study is conducted to investigate morphologies of alpha lactose monohydrate (α LM) grown in polyethylene glycol 300 (PEG 300) solution and vacuum condition via molecular modelling techniques. Surface chemistry of predicted α LM is described. The molecules of α LM in its unit lattice were optimized prior to morphological prediction of attachment energy method and the suitable potential function was determined. The predicted lattice energy of α LM was in excellent agreement with the experimental lattice energy with percent errors of 3.9%. The morphology of α LM is predicted to be hexagonal in shape, similar to crystal morphology of α LM grown in PEG 300 solutions. It was found that the lattice energy and of α LM was dominated by the weak van der Waals force.

Keywords: hydrogen bond; lattice energy molecular modelling; surface chemistry.

1. Introduction

Crystal morphology is an expression of interplay between characteristics of the molecule and external conditions of the molecule is subjected. Experimental molecular morphology depends on the type of solvents and crystallization methods employed, e.g. ibuprofen has various morphologies in different solvent [1]–[3]. Currently, predicted morphology by molecular modelling becomes complementary alternative prior to experimental works. Capability of molecular modelling to mimics the molecule characteristics and external conditions to some degree of accuracy through select morphological models in a faster way is important to produce predicted morphology. This is because not all morphologies, like tabular or platy and acicular are feasible for production in industry. Couple with other capabilities such as cocrystal prediction, molecular modelling is a functional tool in analysis and solution of problems related to crystallization [4].

Fast and reliable prediction of morphology helps in prediction of cocrystal. Validated predicted morphology and corresponding predicted lattice energy is one step forward for cocrystal modelling and drug-excipient screening. Selected predicted morphology will have surface chemistry of its facets evaluated before binding prediction can be carried out. Likewise, the success of cocrystal prediction is validated by experiments proved by the researchers [5]–[8]. Prediction of cocrystal is important because not all methods of crystallization among potential components will yield cocrystal, and hence this has led to several methods of screening cocrystals. Cocrystal method manipulates supramolecular chemistry of drug and coformer molecules to interact intermolecularly [9]. There are numerous potential conformers to fine tune a drug properties which opens up vast possibilities of desired properties [10]. α -lactose monohydrate (α LM), a common excipient, is a potential conformer in GRAs [11]. Lactose in general has high solubility with β -lactose being more soluble than α -lactose [12]–[16]. Crystal stability is important to avoid conversion during storage, clinical use and manufacturing [9]. Crystallization of α LM does

not only yield α -lactose anomer in solutions but also β -anomer, a phenomenon called mutarotation. This is due to the change of a moiety from α -D-Glucose to β -D-Glucose [14]–[19]. The unintended and unwanted species of β -anomer interferes with crystallization of pure α LM to some extent, a condition described as self-poisoning [20]. Other researchers have described self-poisoning in other materials [21]–[24]. This contributes to highly polar, anisotropic morphology of α -lactose monohydrate (α LM) [25]. The resolved structure of this crystal might affect the subsequent computational molecular modelling. The objective of this paper is to predict and validate lattice energy and morphology of lactose and its surface chemistry of facets is evaluated.

2. Materials

2.1. Materials

α -lactose monohydrate ($C_{12}H_{22}O_{11}$) (α LM) powder (Pharmatose 450M, DMV) of 99.99% purity, CAS 64044-51-5. α LM powder is white or almost white, crystalline powder which is soluble in water, but practically insoluble in ethanol and totally insoluble in non-polar solvents. Its molecular weight is 342.30 g/mol. The lactose conforms to pharmacopoeia of USP-NF, Ph.Eur. and J.P. Polyethylene Glycol 300 ($C_{2n}H_{4n+2}O_{n+1}$) (PEG 300) of CAS 25322-68-3, Ph.Eur was obtained from Sigma-Aldrich, Germany. The viscous, clear solvent is soluble in water with average molecular weight of 300 g/mol.

2.2. Crystal structure

The molecular structure of α LM is shown in Fig. 1(a) while the packed molecule in monoclinic lattice with space group $P2_1$ is shown in Fig. 1(b). The two α LM molecules are packed with the same conformation, with the presence of one water molecule in a unit cell. Hence, there is a single α LM molecule in the asymmetric

unit. The cell parameters are $a = 4.7830$; $b = 21.540$, $c = 7.7599$ Å, and $\alpha = \gamma = 90^\circ$, $\beta = 105.911^\circ$.

(a)



An alpha lactose monohydrate molecule (α LM)

(b)

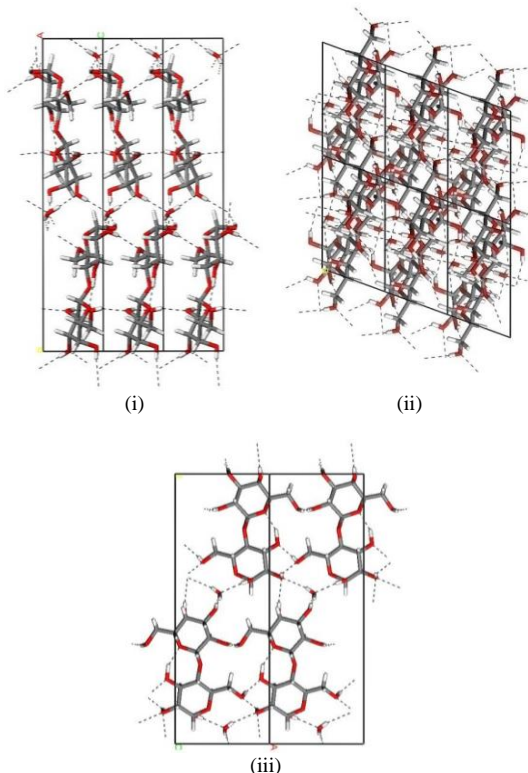


Fig. 1: Molecular structure of (a) $L\alpha \cdot H_2O$ crystal lattice with hydrogen bond network, in the order of: (i) view from x-direction, (ii) view from y-direction and (iii) view from z-direction

The packing involved a complex 3D hydrogen bond network, in which each α -lactose is bonded intermolecularly for 14 hydrogen bonds. Meanwhile, each water molecule is hydrogen-bonded to four different α -lactose molecules [12], [26]. α LM is built from a moiety of β -D-galactose and a moiety of α -D-glucose, joined by a 1,4 glycosidic bond between C1 of galactose and C4' of the glucose unit [18], [19], [26], [27].

3. Method

3.1. Crystallization

Crystallization of α LM in PEG 300 solutions was conducted in which solute and water were added successively into PEG 300 solutions to produce supersaturated solution. Fixed 5 mL PEG solvent, solute and water were mixed in a 100 mL beaker for each crystallization process. The solutions were heated at 80°C , mixed at 1100 rpm using magnetic stirrer on hot-plates. Method of crystallization used was water evaporation and cooling at ambient temperature. The beakers were capped with aluminum foil, punctured with several holes on it so that water vapor could escape from the solution in the beakers.

3.2. Characterization

The polarized light microscope, Olympus BX41 (Olympus, Japan) with magnification powers of 4x, 10x, 20x and 40x were used mainly to observe crystal morphologies. Sample of crystallized solute was placed on a glass slide on a mechanical stage with rotation and translation function. Polarized effect and lighting magnitude sourcing from 6V-30W halogen Kohler lamp, from top and bottom was adjusted to obtain a clear image of crystal morphology.

3.3. Computational details

In this work, a molecular modeling software, (Material Studio 4.4 by Accelrys) was used for the prediction of α LM morphology. α LM molecules of resolved crystal structure were obtained from Cambridge Crystallographic Data Centre (CCDC ID: LAC-TOS10). The simulation was carried out in vacuum environment.

3.3.1. Atomic charges determination

Each atom in α LM molecule was calculated for its charge, corresponding to structure optimization based on a unique density functional theory of quantum mechanical code, an ab-initio method [28]. The geometry α LM molecules was optimized (using delocalized internal coordinates) up to nuclei level so that a stable geometry was produced and hence minimum energy was achieved. This corresponds to refinement of atoms positions in an iterative procedure with maximum step size of 0.3 Å, whereby atoms coordinate was adjusted so that the energy of the structures was brought to a stationary point. In other words, the forces on the atoms were zero. The atomic charge calculation generated atomic charges of Mulliken and Hirshfeld using BLYP-GGA and BLYP-PW91 functions; respectively. Both functions used double numerical plus d-functions (DND) basis set and all electron core treatment.

3.3.2. Morphology prediction and lattice energy determination

The charges set then were assigned into each atom of molecules for the next stage of geometrical optimization. The geometries of α LM molecules in its unit cell were optimized by using selected potential functions (force fields), together with charge set of Mulliken and Hirshfeld. The potential functions used were PCFF and CVFF. The optimization procedures adapted calculated electrostatic and van der Waals forces of the system by Ewald summation. Next, the morphology calculation was performed using attachment energy (AE) method using the same potential functions. Potential energy of the periodic system was calculated by using the Ewald summation for electrostatic and van der Waals force, which make up the components of predicted lattice energies. The predicted lattice energies were compared to the experimental data which was calculated by using equation (1);

$$E_{\text{latt}} = -\Delta H_{\text{sub}} - 2RT \quad (1)$$

where ΔH_{sub} is sublimation enthalpy and $2RT$ represents a correction factor, for the difference between the gas phase enthalpy and the vibrational contribution to the crystal enthalpy [29]–[31]. The lattice energy with the smallest percentage error from the experimental lattice energies indicates that the potential function used is the most suitable to describe the predicted morphology of the system. All surfaces of the faceted morphology α LM were then cleaved for analysis of surface chemistry. The slice energies, E_{slice} for each habit facet were calculated using equation (2);

$$E_{\text{att}} = E_{\text{latt}} - E_{\text{slice}} \quad (2)$$

Lattice energy, E_{latt} or crystal energy is the summation of both attachment energy, E_{att} and slice energy, E_{slice} for a given facet.

4. Results and discussion

4.1. Morphology prediction of alpha lactose monohydrate

The morphology of α LM was simulated in the vacuum condition because the determined facets will be used as surfaces for attachment prediction work. Two types of potential functions were used to simulate α LM morphology, which is PCFF and CVFF. Charges set was calculated independently (not shown) by using Hirshfeld and Mulliken methods before assigning them to the α LM structure. In calculating predicted lattice energy, two types of charge sets were used in this work, i.e., Hirshfeld and Mulliken. The calculated charge sets were then used to calculate lattice energy subjected to potential functions as shown in Table 1. Enthalpy of sublimation, ΔH_{sub} of α LM was taken to be -39.45 kcal/mol. Then, equation (1) was used to calculate the experimental lattice energy, E_{latt} in Table 1.

Table 1: Lattice energies and its associated energies (kcal/mol) of α LM computed using different potential function and charges types. Charge type is sourced from atomic charge calculation.

Potential Function	Charge set	VdW	E _{stat}	E _{latt}	E _{latt} Error (%)
Experimental	-	-	-	-40.3	-
PCFF	Mulliken	-14.9	-	-142.1	252.6
	Hirshfeld	-37.1	-4.7	-41.9	3.9
CVFF	Mulliken	-14.4	-	-168.9	319.3
	Hirshfeld	-29.1	-5.1	-34.2	15.1
Némethy ^a	-	-32.8	-3.4	-36.2 (monomeric model)	10.2
	-	-16.9	-1.8	-18.7 (dimeric model)	53.6
CVFF ^b	-	-	-	-	-

^aClydesdale et al.

^bDincer et al.

The result shows that the experimental lattice energy α LM is -40.2909 kcal/mol and these values were used as the basis for the percentage error calculation. It is found that the calculated lattice energies are sensitive to the charge set as well as potential functions used [32], whereby the predicted lattice energies varies between -34.2 and -168.9 kcal/mol. Comparison between the experimental and predicted lattice energies calculated in Table 1 shows that the percentage deviation varies between 3.9 and 319.3%. Potential functions and charge set which show high deviation of more than 100% from the experimental lattice energy, are not suitable to be used for further modelling calculation. In this work, the difference between predicted and experimental percentage of less than 5% is taken as a good approximation. PCFF force field coupled with Hirshfeld charge set are succeeded in predicting E_{latt} of α LM=-41.9 kcal/mol (3.9% error). Clydesdale, Roberts, Telfer and Grants [33] simulated lattice energy of α LM using two type of model, namely monomeric and dimeric model (Table 1). Dimeric model [33] is similar to model in this work, in which the model sums up the lattice energies for both α -lactose and a water molecule because α LM consists a monohydrate (a water molecule) in crystal lattice. On contrary, monomeric model neglects the interactions between α -lactose and a water molecule [33] which does not mimics well intermolecular interaction in the crystal lattice of α LM. In this work, the contribution of E_{stat} =-4.7 kcal/mol to the E_{latt} =-41.9 kcal/mol is 11.3 %, is relatively low, suggesting that dipolar effects, despite its importance, are not particularly significant in the solid state [33]. The similar trend is also recorded in both monomeric and dimeric model (~10%) [33]. It shows that the predicted lattice energy of α LM in this work, van der Waals energy is dominant which is -37.1 kcal/mol (88.7%) rather than

E_{stat} despite the abundance of hydroxyl groups (-OH) possessed by α LM molecule.

Fig. 2 shows the predicted platy elongated hexagonal morphology of this work simulated in the vacuum condition, hence solvent effect is not considered. The dominant facets are (020) and (0-20), followed by {100}, and both {110} and {1-10} of the same facet area. The predicted shape of this work using CVFF force field (Table 1) is found to be similar to α LM experimental morphologies recovered from PEG 300 solutions of this work (Fig. 3(b)) and α LM crystal morphology by Dincer et al., (1999) in both experiments and modelling.

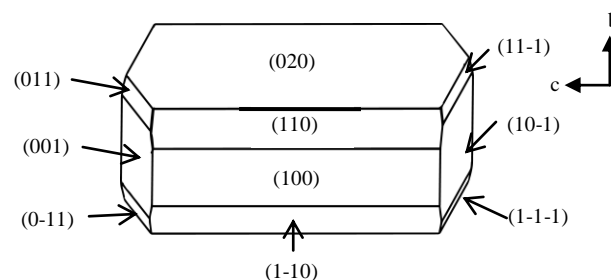


Fig. 2: Predicted elongated hexagonal or prism morphology of lactose using Universal force field with Hirshfeld atomic charges

The similarity between predicted morphology in Fig. 2 and experimental morphology of this work in Fig. 3(b)) is might be due to effect of β -lactose on experimental morphology is small enough although percentage of β -lactose is not measured in this work. Nevertheless, this is evidenced by the same elongated hexagonal morphology or prism obtained by Dincer, Parkinson, Rohl and Ogden [18] in simulation and experiment with presence of 10% β -lactose in DMSO solutions. This might suggest that the effect of 10% β -lactose is negligible on α LM morphology of this work. The low percentage of β -lactose coincides well with high supersaturation ratio of α LM in solution proven by changes of morphology from prism, diamond, pyramid to tomahawk as supersaturation decreases and as mutarotation of α LM progresses into equilibrium at 37% α -lactose and 63% β -lactose [19], [20], [34], [35]. α LM recovered in DMSO solution has considerable growth in c -direction and some growth in a -direction, with most rapid growth observed at $\{011\}$ and $\{101\}$ facets [18]. Lattice parameters (a, b, c) of the predicted morphology in this work (Fig. 2) are similar to this experimental (Fig. 3(b)) and modelling of Dincer, Parkinson, Rohl and Ogden [18].

Clydesdale, Roberts, Telfer and Grants [33] are the first researchers predicting tomahawk morphology, using Némethy force field (Table 1). However, some facets are lost and not tapered at one end (b -direction) compared to schematic morphology of Dincer, Ogden and Parkinson [36] and experimental morphology of this work (Fig. 3(a)) recovered from aqueous solutions.

Suitable force field and charge is not the only factor contributing to similarity of predicted to experimental morphology. Another factor which is often overlooked is the crystal structure of α LM itself. The structure used in this work was determined to have as small as 7% of β -anomer. This impurity was derived from feed crystals recovered from aqueous solutions via slow evaporation crystallization, presumably at room temperature [26]. β -anomer might be included in the lattice of feed crystals and affects the determined structure used in this work. Smith, Dann, Elsegood, Dale and Blathford [27] also noted that there was β -anomer presence with unclosed percentage in their determined structure of α LM [27]. The feed crystals were recovered from a mixture of 10% lactose solution and acetone in a ratio of 35:65 in which crystallization occur at room temperature.

This implies that the determined molecular structures by Fries, Rao and Sundaralingam [26] and Smith, Dann, Elsegood, Dale and Blathford [27]) are not free from β -anomer impurity. This

impurity affects the molecular structure to some extent, although the presence of 7% of β -anomer can be negligible.

During the course of molecular modelling on morphology of α LM in this work, the morphological modelling does not convert any α -lactose structures into β -lactose (mutarotation process) since doing so would be similar to additive calculation in the modelling. Thus, α LM structure remains with inherent 7% of β -anomer. However, in terms of mimicking mutarotation, the molecular modelling failed to take account of mutarotation process.

The tomahawk morphology in Fig. 3(a) shows that α LM grows in b -direction as β -lactose poisons the growth of either (0-20) or (0-10) at the base and (0 $\bar{1}1$) and (0 $\bar{1}\bar{1}$) slanting facets, slowing the facets growth [18], [25].

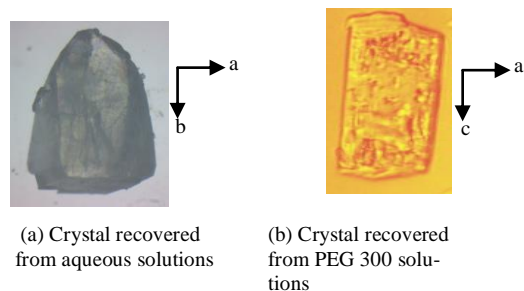


Fig. 3: Tomahawk morphology of α LM in (a) and platy elongated hexagonal or prism morphology in (b).

β -lactose is unable to poison the (010) surface of tomahawk morphology due to galactose end of α LM lies at the surface [26], [36]. It is believed that the experimental elongated platy hexagonal α LM crystal by Dincer, Parkinson, Rohl and Ogden [18] shares the same growth changes with β -lactose content (w/w%) as reported by Raghavan, Ristic, Reen and Sherwood [25]. Crystal growth in DMSO and aqueous solution shows that at below 15% β -lactose, both show elongated platy hexagonal habit [18], [25]. As β -lactose content increases, that β -monomer poisons the growth of c -direction which has the fastest growth [18], [25]. This results in faster growth, in b -direction, until there is 40-60% β -lactose in solutions [18], [25]. The percentage approaches the equilibrium mutarotation of α and β anomer which is \sim 40:60 (w/w) [19], normally present in solutions favouring tomahawk morphology.

4.2 Surface chemistry analysis

Table 2 shows details of attachment and slice energy with respect to crystal face calculated using attachment energy (AE) method. The slice energy was computed using equation 2.

In Table 2, there are eleven visible habit facets, similar to those found in the predicted morphology of α LM by Dincer, Parkinson, Rohl and Ogden [18] except (10 $\bar{1}$). Based on the premise of low electrostatic energy, Est corresponds to high possibility of binding sites in Table 2, it is speculated that there are 4 groups of facets with possible binding sites. From decreasing order of possibility, group 1 of highest possibility consists of {100}, {110} and { $\bar{1}10$ } facet at Est more than 3.00 kcal/mol. This followed by group 2 at Est=-2.50 kcal/mol consisting of {001}, {011} and {0 $\bar{1}1$ } facets.

Group 3 with Est more than -1.60 kcal/mol comprises of {10 $\bar{1}$ }, { $\bar{1}10$ } and { $\bar{1}\bar{1}1$ } facets. The lowest possibility of binding site of group 4 comprises of both (020) and (0 $\bar{2}0$) facets. Due to those possible binding sites and influence from hydroxyl orientation and intramolecular hydrogen bonding of alpha lactose and water molecules, possible different morphology of lactose might be produced. All habit facets in Table 2 are polar, evident from Fig. 4 showing exposed oxygen of hydroxyl at crystal surface. The dominating facets of (020) and (0 $\bar{2}0$) have the most maximum attachment

energy of -12.09 kcal/mol each (Table 2) which is the slowest growing faces. This can be observed from the surface chemistry of the large (020) and (0 $\bar{2}0$) faces (Fig. 4(a)(b)) in which α LM molecules are stacked vertically, limiting exposure of potential oxygen atoms for interaction. The facets of {011} (Fig. 4(j)) are with the most minimum attachment energy, resulting in fast growth and hence morphologically less important. It is found that when α LM molecules with pyranose rings facing upward the crystal boundary, the corresponding facets of surface chemistry in Fig. 4(f)-(k) such as {10 $\bar{1}$ }, {001}, { $\bar{1}10$ }, { $\bar{1}\bar{1}1$ }, (011) and {0 $\bar{1}1$ } have minimum attachment energy compared to the rest, resulting in a fast growth and less morphological important facets. Thus, it is vice-versa for the remaining facets which is (020), (0 $\bar{2}0$), {100}, {110} and { $\bar{1}10$ } (Fig. 4(a)-(e)).

Table 2: Facet, multiplicity and d-spacing from attachment energy, AE method using PCFF force field with Hirshfeld atomic charges showing the respective attachment and slice energy. All energies in kcal/mol.

Habit facet	Multiplicity	d-spacing	E_{slice}	E_{att} (total)	E_{att} (vdW)	E_{att} (Est)
(020)	1	10.8	-29.77	-12.09	-11.49	-0.60
(0 $\bar{2}0$)	1	10.8	-29.77	-12.09	-11.49	-0.60
{100}	2	7.5	-24.48	-17.38	-13.68	-3.71
{110}	2	7.1	-23.62	-18.25	-15.00	-3.24
{ $\bar{1}10$ }	2	7.1	-23.62	-18.25	-15.00	-3.24
{10 $\bar{1}$ }	2	4.6	-14.00	-27.90	-26.30	-1.60
{001}	2	4.5	-12.50	-29.40	-26.90	-2.50
{ $\bar{1}10$ }	2	4.5	-12.65	-29.20	-27.40	-1.80
{ $\bar{1}\bar{1}1$ }	2	4.5	-12.65	-29.20	-27.40	-1.80
{011}	2	4.4	-11.39	-30.50	-28.00	-2.50
{0 $\bar{1}1$ }	2	4.4	-11.39	-30.50	-28.00	-2.50

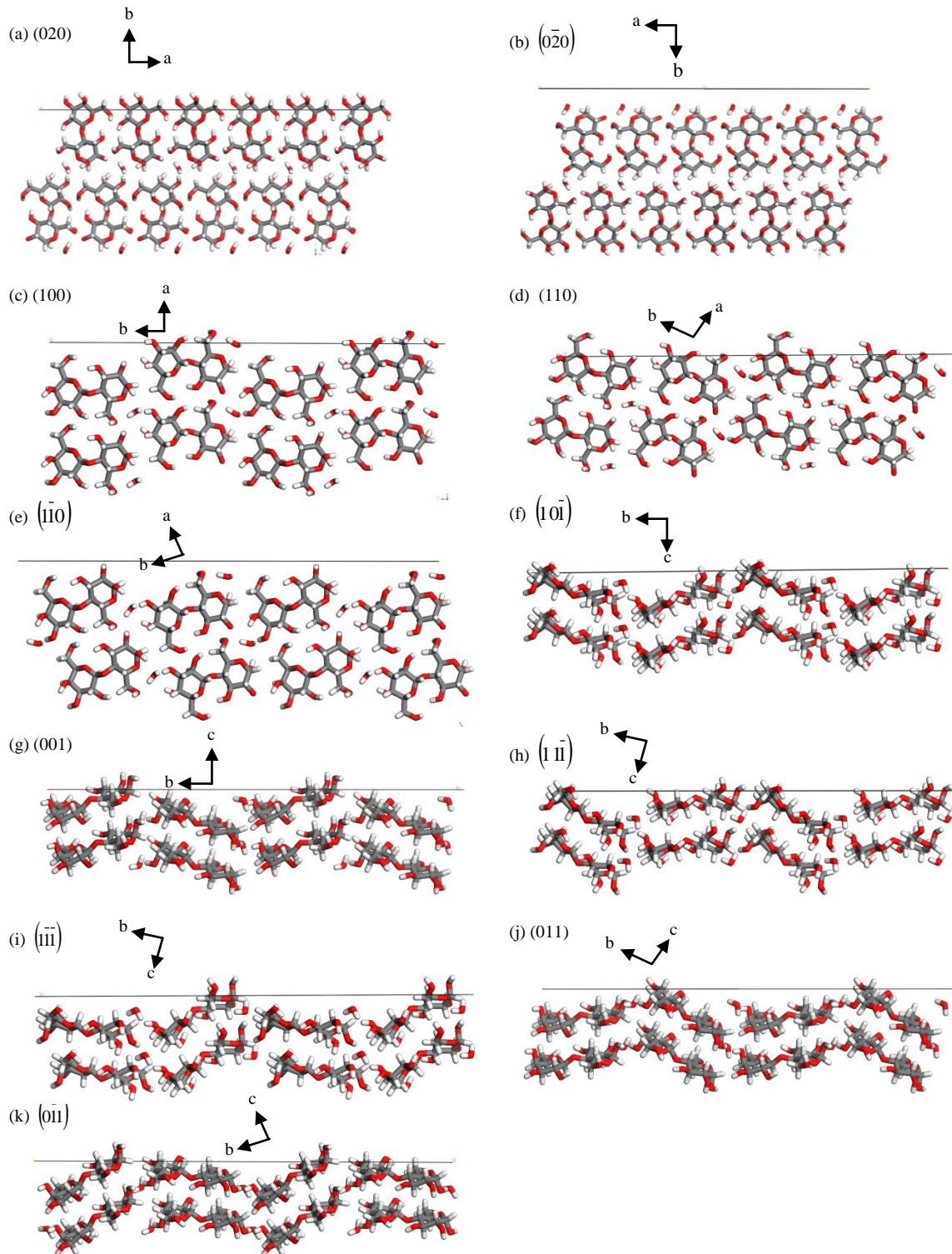


Fig. 4: Molecular packing diagram of $L\alpha.H_2O$, illustrating the surface chemistry of crystal faces: (a) (020) (b) $(0\bar{2}0)$ (c) (100) (d) (110) (e) $(\bar{1}\bar{1}0)$ (f) $(10\bar{1})$ (g) (001) (h) $(1\bar{1}\bar{1})$ (i) $(\bar{1}\bar{1}\bar{1})$ (j) (011) (k) $(0\bar{1}\bar{1})$ using PCFF and Hirshfeld charge set.

5. Conclusion

Predicted lattice energy of alpha-lactose monohydrate (-41.9 kcal/mol) calculated with PCFF force field coupled with Hirshfeld charge set recorded the lowest error of lattice energy, 3.9%. The subsequent predicted morphology and experimental agrees well with others for both predicted and experimental works. Molecular

structure of lactose is, to some extent, not free of β -anomer impurity being incorporated into its structure. Based on possible binding sites, β -anomer impurity are likely to incorporate at $\{100\}$, $\{110\}$ and $\{\bar{1}10\}$ facets.

Acknowledgement

The authors would like to express their gratitude to the Ministry of Higher Education (MOHE), Malaysia for funding of this work. This work is part of grant 600-RMI/MyRA 5/3/BESTARI (023/2017).

References

- [1] N. Rasenack and B. W. Müller, "Ibuprofen crystals with optimized properties", *International Journal of Pharmacy*, Vol.45, (2002), pp.9–24.
- [2] N. Rasenack & B. W. Müller, "Properties of ibuprofen crystallized under various conditions: a comparative study", *Drug Development and Industrial Pharmacy*, Vol.28, No.9, (2002), pp.1077–1089.
- [3] H. Cano, N. Gabas & J. P. Canselier, "Experimental study on the ibuprofen crystal growth morphology in solution," *Journal of Crystal Growth*, Vol.224, No.3, (2001), pp.335–341.
- [4] A. S. Myerson, *Molecular Modeling Applications in Crystallization*, Cambridge University Press, (1999), pp:106–160.
- [5] A. J. Cruz Cabeza, G. M. Day, W. D. S. Motherwell & W. Jones, "Prediction and observation of isostructurality induced by solvent incorporation in multicomponent crystals," *Journal of American Chemical Society*, Vol.128, No.45, (2006), pp.4466–14467.
- [6] N. Issa, P. G. Karamertzanis, G. W. A. Welch, and S. L. Price, "Can the formation of pharmaceutical cocrystals be computationally predicted? i. comparison of lattice energies," *Crystal Growth & Design*, Vol.9, No.1, (2009), pp.442–453.
- [7] P. G. Karamertzanis, A. V. Kazantsev, N. Issa, G. W. A. Welch, C. S. Adjiman, C. C. Pantelides, and S. L. Price, "Can the formation of pharmaceutical cocrystals be computationally predicted? 2. crystal structure prediction," *Journal of Chemical Theory & Computation*, Vol.5, No.5, (2009), pp.1432–1448.
- [8] A. Lemmerer, C. Esterhuysen, and J. Bernstein, "Synthesis, characterization, and molecular modeling of a pharmaceutical cocrystal: (2-chloro-4-nitrobenzoic acid):(nicotinamide)," *Journal of Pharmaceutical Science*, Vol.99, No.9, (2010), pp.4054–4071.
- [9] O. Almarsson and M. J. Zaworotko, "Crystal engineering of the composition of pharmaceutical phases. Do pharmaceutical cocrystals represent a new path to improved medicines?," *Chemical Communications*, No.17 (2004), pp.1889–1896.
- [10] J. Y. Sabiruddin Mirza, Inna Miroshnyk, Jyrki Heinämäki, "Cocrystals: an emerging approach for enhancing properties of pharmaceutical solids," *Dosis*, Vol.24, (2008), pp.90–96.
- [11] J. Chen, B. Sarma, J. M. Evans, and A. S. Myerson, "Pharmaceutical crystallization: published as part of the Crystal Growth & Design 10th anniversary perspective," *Crystal Growth & Design*, Vol.11, (2011), pp.887–895.
- [12] S. Garnier, S. Petit, and G. Coquerel, "Influence of supersaturation and structurally related additives on the crystal growth of α -lactose monohydrate," *Journal of Crystal Growth*, Vol.234, No.1, (2002), pp.207–219.
- [13] J. J. B. Machado, J. A. Coutinho, and E. A. Macedo, "Solid–liquid equilibrium of α -lactose in ethanol/water", *Fluid Phase Equilibria*, Vol.173, (2000), pp.121–134.
- [14] P. F. Fox, T. Uniacke-Lowe, P. L. H. McSweeney, and J. A. O'Mahony, *Dairy Chemistry and Biochemistry*. Springer International Publishing, (2015), pp:27–30.
- [15] N. Board, *The Complete Technology Book on Dairy & Poultry Industries With Farming and Processing*, (2012), pp:344–345.
- [16] B. K. Simpson, L. M. L. Nollet, F. Toldrá, S. Benjakul, G. Paliyath, and Y. H. Hui, *Food Biochemistry and Food Processing*. Wiley, (2012), pp:444–445.
- [17] S. Garnier, S. Petit, and G. Coquerel, "Dehydration mechanism and crystallisation behaviour of lactose," *Journal of Thermal Analysis*, Vol. 68 (2002), pp.489–502.
- [18] T. D. Dincer, G. M. Parkinson, A. L. Rohl, and M. I. Ogden, "Crystallisation of α -lactose monohydrate from dimethyl sulfoxide (DMSO) solutions: influence of β -lactose," *Journal of Crystal Growth*, Vol.205, (1999), pp.368–374.
- [19] P. MacFhionnghaile, V. Svoboda, J. McGinty, A. Nordon, and J. Sefcik, "Crystallization diagram for antisolvent crystallization of lactose: using design of experiments to investigate continuous mixing-induced supersaturation," *Crystal Growth & Design*, Vol.17, No.5, (2017), pp. 2611–2621.
- [20] P. Parimaladevi and K. Srinivasan, "Influence of supersaturation level on the morphology of α -lactose monohydrate crystals," *International Dairy Journal*, Vol.39, (2014), pp.301–311.
- [21] X. Liu, E. Boek, W. Briels, and P. Bennema, "Analysis of morphology of crystals based on identification of interfacial structure," *Journal of Chemical Physics*, Vol.103, No.3747, (1995), pp.3747–3754.
- [22] C. S. Towler, R. J. Davey, R. W. Lancaster, and C. J. Price, "Impact of molecular speciation on crystal nucleation in polymorphic systems: the conundrum of gamma glycine and molecular 'self poisoning'." *Journal of American Chemical Society*, Vol.126, No.41, (2004), pp.13347–13353.
- [23] C. Stoica, P. Tinnemans, H. Meekes, W. J. P. van Enkevort, and E. Vlieg, "Rough growth behavior of a polar steroid crystal: a case of polymorphic self-poisoning?," *Crystal Growth & Design*, Vol.6, No.6, (2006), pp.1311–1317.
- [24] I. Weissbuch, L. Leiserowitz, and M. Lahav, "Self-poisoning at $\{011\}$ faces of α -resorcinol crystals may explain its unidirectional growth in the vapor phase: a molecular modeling study," *Crystal Growth & Design*, Vol.6, No.3, (2006), pp.625–628.
- [25] S. L. Raghavan, R. I. Ristic, D. B. Sheen, and J. N. Sherwood, "Morphology of crystals of α -lactose hydrate grown from aqueous solution," *Journal of Physical Chemistry B*, Vol.104, (2000), pp.12256–12262.
- [26] D. C. Fries, S. T. Rao, and M. Sundaralingam, "Structural chemistry of carbohydrates. iii. crystal and molecular structure of 4- α - β -D-galactopyranosyl- α -D-glucopyranose monohydrate (α -lactose monohydrate)," *Acta Crystallographica Section B*, Vol.B27, (1971), pp.994–1005.
- [27] J. H. Smith, S. E. Dann, M. R. J. Elsegood, S. H. Dale, and C. G. Blatchford, " α -lactose monohydrate: a redetermination at 150 K," *Acta Crystallographica Section E*, Vol.61, No.8, (2005), pp.2499–2501.
- [28] J. C. Givand, R. W. Rousseau, and P. J. Ludovice, "Characterization of l-isoleucine crystal morphology from molecular modeling," *Journal of Crystal Growth*, Vol.194, No.2, (1998), pp.228–238.
- [29] V. Bisker-Leib and M. F. Doherty, "Modeling the crystal shape of polar organic materials: prediction of urea crystals grown from polar and nonpolar solvents," *Crystal Growth & Design*, Vol.1, No.6, (2001), pp.455–461.
- [30] D. H. Dressler, I. Hod, and Y. Mastai, "Stabilization of α -l-glutamic acid on chiral thin films—a theoretical and experimental study," *Journal of Crystal Growth*, Vol.310, (2008), pp.1718–1724.
- [31] S. K. Poornachary, P. S. Chow, and R. B. H. Tan, "Impurity effects on the growth of molecular crystals: experiments and modeling," *Advanced Powder Technology*, Vol.19, (2008), pp.459–473.
- [32] S. K. Poornachary, P. S. Chow, and R. B. H. Tan, "Effect of solution speciation of impurities on α -glycine crystal habit: a molecular modeling study," *Journal of Crystal Growth*, Vol.310, No.12, (2008), pp.3034–3041.
- [33] G. Clydesdale, K. J. Roberts, G. B. Telfer, and D. J. W. Grant, "Modeling the crystal morphology of α -lactose monohydrate," *Journal of Pharmaceutical Science*, Vol.86, No.1, (1997), pp.135–141.
- [34] A. Paterson, "Lactose processing: from fundamental understanding to industrial application," *International Dairy Journal*, Vol.67, (2017), pp.80–90.
- [35] A. Xun, T. Truong, and B. Bhandari, "Effect of Carbonation of supersaturated lactose solution on crystallisation behaviour of alpha-lactose monohydrate," *Food Biophysics*, Vol.12, (2017), pp.52–59.
- [36] T. D. Dincer, M. I. Ogden, and G. M. Parkinson, "In situ investigation of growth rates and growth rate dispersion of α -lactose monohydrate crystals," *Journal of Crystal Growth*, Vol.311, (2009), pp.1352–1358.